BIOMOLECULES & THERAPEUTICS

Original Article
Biomol Ther 23(2), 165-173 (2015)

Galangin (3,5,7-Trihydroxyflavone) Shields Human Keratinocytes from Ultraviolet B-Induced Oxidative Stress

Susara Ruwan Kumara Madduma Hewage[1], Mei Jing Piao[1], Ki Cheon Kim[1], Ji Won Cha[1], Xia Han[1], Yung Hyun Choi[2], Sungwook Chae[3] and Jin Won Hyun[1,*]

[1]Jeju National University School of Medicine, Jeju 690-756, [2]Department of Biochemistry, College of Oriental Medicine, Dongeui University, Busan 614-052, [3]Aging Research Center, Korea Institute of Oriental Medicine, Daejeon 305-811, Republic of Korea

Abstract

Most skin damage caused by ultraviolet B (UVB) radiation is owing to the generation of reactive oxygen species. Phytochemicals can act as antioxidants against UVB-induced oxidative stress. This study investigated the protective effects of the flavone galangin against UVB-induced oxidative damage in human keratinocytes. Galangin efficiently scavenged free radicals and reduced UVB-induced damage to cellular macromolecules, such as DNA, lipids, and proteins. Furthermore, galangin rescued cells undergoing apoptosis induced by UVB radiation *via* recovering mitochondrial polarization and down-regulating apoptotic proteins. These results showed that galangin protects human keratinocytes against UVB radiation-induced cellular damage and apoptosis *via* its antioxidant effects.

Key Words: Apoptosis, Galangin, Human keratinocytes, Oxidative damage, Ultraviolet B

INTRODUCTION

Solar radiation can be divided into three main types based on its wavelength, namely, ultraviolet (UV), visible light, and infrared (Lyons and O'Brien, 2002). Of these, UV radiation is the most responsible for photoaging and skin cancer. UV radiation is subdivided into UVA (320-400 nm), UVB (280-320 nm), and UVC (200-280 nm). The ozone layer reflects UVC radiation, meaning only UVA and UVB reach the earth's surface. UVB radiation is particularly absorbed by human skin and causes erythema, burns, immune suppression, and skin cancer (Park *et al*., 2013). Although UVA accounts for the majority of UV radiation that reaches the earth's surface and can penetrate the skin deeper than UVB, it is weakly carcinogenic and causes aging and wrinkling of the skin (Yoshikawa *et al*., 1990; Donawho *et al*., 1996; Matsumura and Ananthaswamy, 2004).

UVB directly or indirectly damages skin cells *via* the formation of cyclobutane pyrimidine dimers (CPDs) and pyrimidine-pyrimidone(6-4) photoproducts or *via* the generation of reactive oxygen species (ROS), such as hydroxyl radicals (•OH), superoxide anions ($\bullet O_2^-$), hydrogen peroxide (H_2O_2), and singlet oxygen ($^1O_2$) (Cunningham *et al*., 1985; Hattori *et al*., 1996; Meeran *et al*., 2008). UVB-exposed cells generate ROS by activating specific small molecules such as riboflavin, tryptophan, and porphyrin (Ikehata and Ono, 2011). The antioxidant defense system in cells balances ROS production; however, when levels of ROS are elevated, this antioxidant defense system is overwhelmed, resulting in oxidative stress. Uncontrolled release of ROS causes single- and double-strand DNA breaks and DNA-protein cross-linking (Caldwell *et al*., 2007). ROS also attack important cellular structural and functional molecules, such as lipids and proteins, causing the malfunction of cellular activities, finally leading to apoptosis, a process of programmed cell death (Tsoyi *et al*., 2008; Dhumrongvaraporn and Chanvorachote, 2013).

With the increased occurrence of skin cancers and other damaging effects of UVB exposure, the protection of skin from UVB-induced oxidative cellular damage has become a key consideration in the pharmaceutical industry. Phytochemicals are well-known for their protective effects against oxidative stress in the skin (Sumiyoshi and Kimura, 2009). Galangin (3,5,7-trihydroxyflavone, Fig. 1) is a type of flavonoid that is commonly found in *Alpinia officinarum* and *Helichrysum aureonitens* (Afolayan and Meyer, 1997; Ciolino and Yeh, 1999). Galangin has antibacterial (Cushnie and Lamb, 2005; 2006)

Open Access **http://dx.doi.org/10.4062/biomolther.2014.130**

Received Nov 25, 2014 **Revised** Jan 13, 2015 **Accepted** Jan 20, 2015
Published online Mar 1, 2015

***Corresponding Author**
E-mail: jinwonh@jejunu.ac.kr
Tel: +82-64-754-3838, Fax: +82-64-702-2687

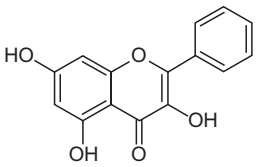

Fig. 1. Chemical structure of galangin (3,5,7-trihydroxyflavone).

and antiviral (Afolayan *et al*., 1997) properties and suppresses breast tumor cell growth (So *et al*., 1996; Diffey, 2004). However, the cytoprotective effects of galangin against UVB-induced oxidative damage in human keratinocytes have not been studied. Therefore, the objective of this study was to investigate the protective effects of galangin against UVB-induced oxidative stress in human keratinocytes.

MATERIALS AND METHODS

Reagents

Galangin was purchased from Santa Cruz Biotechnology Inc. (Dallas, TX, USA). [3-(4,5-Dimethylthiazol-2-yl)-2,5-diphenyltetrazolium] bromide (MTT), 1,1-diphenyl-2-picrylhydrazyl (DPPH), N-acetyl cysteine (NAC), 5,5-dimethyl-1-pyrroline-N oxide (DMPO), 2',7'-dichlorodihydrofluorescein diacetate (DCF-DA), and Hoechst 33342 were purchased from Sigma-Aldrich Inc. (St. Louis, MO, USA). 5,5',6,6'-Tetrachloro-1,1',3,3'-tetraethyl-benzimidazolylcarbocyanine iodide (JC-1) was purchased from Invitrogen (Carlsbad, CA, USA). Primary antibodies for Bax and Bcl-2 were purchased from Santa Cruz Biotechnology Inc. (Dallas, TX, USA). Primary antibodies for caspase-3 and caspase-9 were purchased from Cell Signaling Technology (Danvers, MA, USA). All other chemicals and reagents were of analytical grade.

Cell culture and UVB exposure

The human keratinocyte cell line HaCaT was obtained from Amore Pacific Company (Yongin, Korea) and maintained at 37°C in an incubator with a humidified atmosphere of 5% CO_2. Cells were cultured in RPMI 1640 medium containing 10% heat-inactivated fetal bovine serum, streptomycin (100 μg/ml), and penicillin (100 units/ml). Cells were exposed to UVB at a dose of 30 mJ/cm^2. The CL-1000M UV Crosslinker (UVP, Upland, CA, USA) was used as the UVB source and delivered a UVB energy spectrum of 280-320 nm.

Cell viability assay

The influence of galangin on cell viability was examined using the MTT assay. Cells were seeded in a 96-well plate at a density of 1×10^5 cells/ml. After 24 h, galangin was added to a final concentration of 20, 40, 80, or 100 μM and cells were incubated for 24 h. MTT stock solution (50 μl, 2 mg/ml) was added to each well to yield a final reaction volume of 200 μl. The supernatant was aspirated 4 h later and formazan crystals were dissolved in 150 μl of dimethylsulfoxide (DMSO). The absorbance at 540 nm was read using a scanning multiwell spectrophotometer (Carmichael *et al*., 1987).

Detection of DPPH radicals

The ability of galangin to scavenge DPPH radicals was assessed. Cells in a 96-well plate were treated with 20, 40, 80, or 100 μM of galangin or 1 mM of NAC. DPPH dissolved in ethanol (0.1 mM) was added to each well to yield a total volume of 200 μl. After shaking for 3 h, unreacted DPPH was detected by measuring the absorbance at 520 nm using a spectrophotometer.

Detection of hydroxyl radicals

Hydroxyl radicals generated by the Fenton reaction (H_2O_2+ $FeSO_4$) were reacted with DMPO. The resultant DMPO/•OH adducts were detected using an electron spin resonance (ESR) spectrometer (Li *et al*., 2004). The ESR spectrum was recorded 2.5 min after a phosphate buffer solution (pH 7.4) was mixed with 0.02 ml each of 0.3 M DMPO, 10 mM $FeSO_4$, 10 mM H_2O_2, and 40 μM of galangin. The ESR spectrometer parameters were set as follows: central magnetic field, 336.8 mT; power, 1.00 mW; frequency, 9.4380 GHz; modulation width, 0.2 mT; amplitude, 600; sweep width, 10 mT; sweep time, 0.5 min; time constant, 0.03 sec; and temperature, 25°C.

Detection of intracellular ROS

DCF-DA fluorescence was detected to measure intracellular ROS generated by H_2O_2 or UVB (Rosenkranz *et al*., 1992). Cells were seeded at a density of 1.5×10^5 cells/ml and incubated at 37°C for 24 h. Galangin (40 μM) or NAC (1 mM) was added to each well. After 1 h, cells were treated with H_2O_2 (1 mM) or exposed to UVB. After 30 min, H_2O_2-treated cells were treated with DCF-DA (25 μM) and incubated for another 20 min. UVB-treated cells were incubated for 24 h, treated with DCF-DA (50 μM), and incubated for a further 30 min. Fluorescence of 2',7'-dichlorofluorescein (DCF) was detected and quantified using a PerkinElmer LS-5B spectrofluorometer (PerkinElmer, Waltham, MA, USA). Intracellular ROS scavenging effect of galangin (%)=(absorbance of control cells - absorbance of galangin- or NAC-treated cells)/absorbance of control cells×100. Only H_2O_2-or UVB-treated cells were considered as controls.

Single cell gel electrophoresis (Comet assay)

DNA damage caused by oxidative stress was detected by the comet assay (Singh, 2000; Rajagopalan *et al*., 2003). Cells were seeded at a density of 1×10^5 cells/ml and incubated at 37°C for 24 h. Cells were treated with galangin (40 μM) and after 1 h, exposed to UVB (30 mJ/cm^2). The cell suspension was collected and mixed with 120 μl of 0.7% low melting agarose (LMA) at 37°C. The mixture was spread on a fully frosted microscope slide pre-coated with 200 μl of 1% normal melting agarose. After this had solidified, a further 170 μl of LMA was applied to the slide. Slides were immersed in lysis solution (2.5 M NaCl, 100 mM Na-EDTA, 10 mM Tris, 1% Trion X-100, and 10% DMSO, pH 10) for 90 min at 4°C. Slides were then immersed in an unwinding buffer (300 mM NaOH and 10 mM Na-EDTA, pH 13) for 30 min at 4°C. Slides were subjected to electrophoresis in unwinding buffer solution with an electrical field of 300 mA and 25 V for 20 min at room temperature. The slides were washed three times with neutralizing buffer (0.4 M Tris, pH 7.5) for 10 min each time and then washed with 70% ethanol for 5 min. Slides were stained with 70 μl of ethidium bromide and observed under a fluorescence microscope using an image analyzer (Kinetic Imaging, Komet 5.5, UK). The tail length and the percentage of fluorescence in comet tails were recorded for 50 cells per slide.

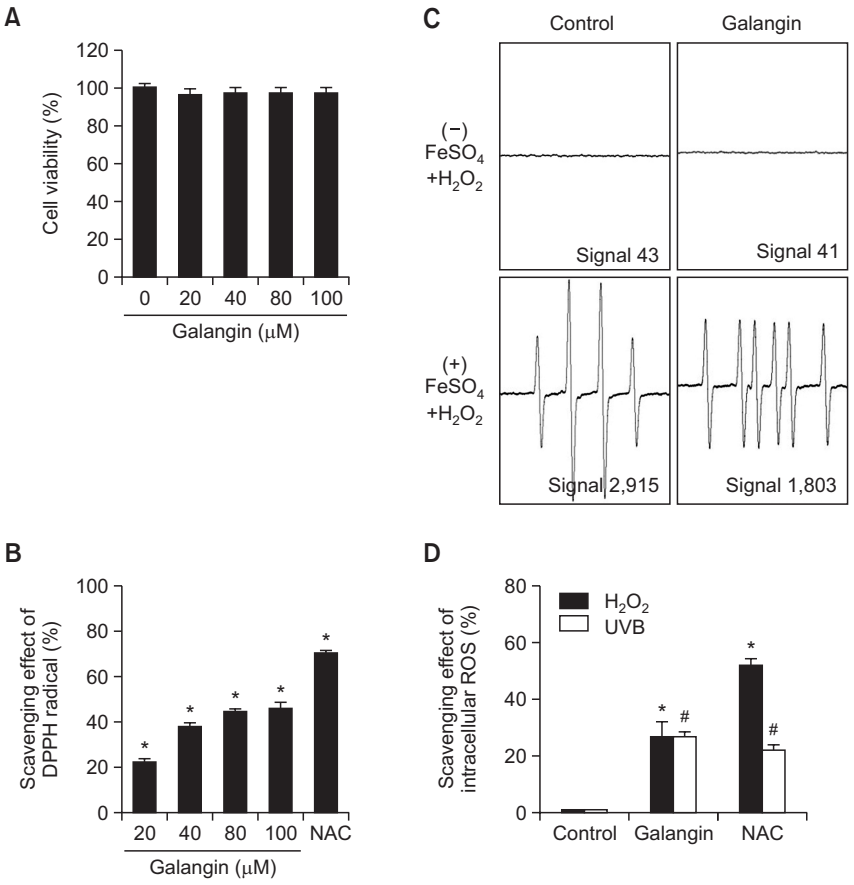

Fig. 2. Galangin scavenges reactive oxygen species (ROS). (A) HaCaT cells were treated with various concentrations of galangin for 24 hours and cell viability was measured by the [3-(4,5-dimethylthiazol-2-yl)-2,5-diphenyltetrazolium] bromide (MTT) assay. (B) Levels of the 1-diphenyl-2-picrylhydrazyl (DPPH) radical were measured spectrophotometrically at 520 nm. N-acetyl cysteine (NAC, 1 mM) was used as the positive control. *Significantly different from the control group (p<0.05). (C) Hydrodroxyl radical-scavenging ability was evaluated using the Fenton reaction system. (D) The ability of galangin to scavenge intracellular ROS generated by H_2O_2 or UVB was assessed using a spectrofluorometer after DCF-DA staining. *,#Significantly different from cells treated with H_2O_2 or UVB alone (p<0.05).

8-Isoprostane assay

Cells were seeded at a density of 1×10^5 cells/ml and incubated at 37°C for 24 h. Cells were treated with galangin (40 μM) and after 1 h, exposed to UVB (30 mJ/cm^2), and incubated at 37°C for another 24 h. Lipid peroxidation was assayed by colorimetric determination of the amount of 8-isoprostane secreted into the culture medium by HaCaT keratinocytes (Beauchamp *et al*., 2002). A commercial enzyme immunoassay (Cayman Chemical, Ann Arbor, MI, USA) was used according to the manufacturer's instructions.

Protein carbonylation assay

Cells were seeded at a density of 1×10^5 cells/ml and incubated at 37°C for 24 h. Cells were treated with galangin (40 μM) and after 1 h, exposed to UVB (30 mJ/cm^2), and incubated at 37°C for another 24 h. The extent of protein carbonyl formation was determined using an OxiSelect™ Protein Carbonyl ELISA Kit from Cell Biolabs (San Diego, CA, USA) according to the manufacturer's instructions.

Nuclear staining with Hoechst 33342

Cells were seeded at a density of 1×10^5 cells/ml and incubated at 37°C for 24 h. Cells were treated with galangin (40 μM) and after 1 h, exposed to UVB (30 mJ/cm^2), and incubated at 37°C for another 24 h. The DNA-specific fluorescent dye Hoechst 33342 was added to each well and cells were incubated for 10 min at 37°C. Stained cells were visualized under a fluorescence microscope equipped with a CoolSNAP-Pro color digital camera. The degree of nuclear condensation was evaluated and apoptotic cells were counted.

Analysis of mitochondrial membrane potential ($\Delta\psi_m$)

JC-1 was added to each well and cells were incubated for 30 min at 37°C. Stained cells were washed with phosphate-buffered saline (PBS), coverslips were mounted onto microscope slides in mounting medium (DAKO, Carpinteria, CA, USA), and slides were examined using a confocal microscope. Microscopic images were collected using the Laser Scanning Microscope 5 PASCAL program (Carl Zeiss, Jena, Germany) (Cossarizza *et al*., 1993). In addition, mitochondrial membrane potential was analyzed by flow cytometry. Cells were harvested, washed, suspended in PBS containing JC-1 (10 μg/ml), incubated for 30 min at 37°C, and analyzed using a flow cytometer (Troiano *et al*., 2007).

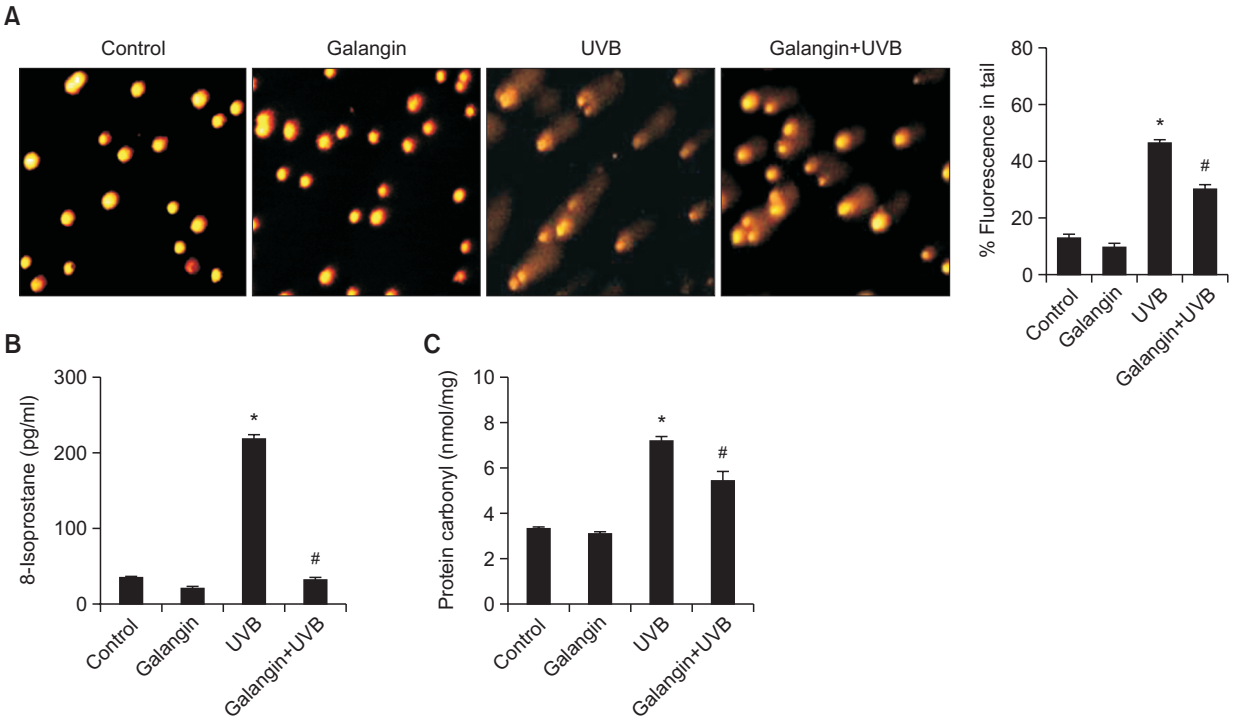

Fig. 3. Galangin attenuates UVB-induced macromolecule damage. Cells were treated with 40 μM of galangin and exposed to UVB (30 mJ/cm^2) 1 hour later. After 24 hours, (A) The comet assay was performed to assess DNA damage. Representative images and the percentage of cellular fluorescence within comet tails are shown. *Significantly different from control cells (p<0.05); #significantly different from UVB only-exposed cells (p<0.05). (B) Lipid peroxidation was assessed by measuring the concentration of 8-isoprostane in the conditioned medium. *Significantly different from control cells (p<0.05); #significantly different from UVB only-exposed cells (p<0.05). (C) Protein oxidation was determined by measuring the amount of carbonyls formed. *Significantly different from control cells (p<0.05); #significantly different from UVB only-exposed cells (p<0.05).

Western blot analysis

Harvested cells were lysed by incubation on ice for 10 min in 150 μl of lysis buffer containing 120 mM NaCl, 40 mM Tris (pH 8), and 0.1% NP 40. The resultant cell lysates were centrifuged at 13,000 rpm for 5 min. Supernatants were collected and protein concentrations were determined. Aliquots were boiled for 5 min and electrophoresed on 12% SDS-polyacrylamide gels. Protein blots of the gels were transferred onto nitrocellulose membranes. The membranes were incubated with the appropriate primary antibodies (1:1,000) followed by horseradish peroxidaseconjugated anti-IgG secondary antibodies (1:5,000) (Pierce, Rockford, IL, USA). Protein bands were detected using an enhanced chemiluminescence Western blotting detection kit (Amersham, Little Chalfont, Buckinghamshire, UK).

Statistical analysis

All measurements were performed in triplicate and all values are expressed as means ± standard error. The results were subjected to an analysis of variance using Tukey's test to analyze differences between means. In each case, a p-value of <0.05 was considered statistically significant.

RESULTS

Galangin attenuates UVB-induced ROS generation

The MTT assay showed that galangin was not toxic to HaCaT cells at any concentration used. Following the treatment with each of the concentrations of galangin tested, cell viability was more than 96% of that of control cells (Fig. 2A). Galangin showed DPPH radical-scavenging activity at concentrations of 20-100 μM compared to treatment with NAC (1 mM), a well-known antioxidant (Fig. 2B). Therefore, 40 μM was selected as the optimal concentration of galangin for further experiments. To assess the ability of galangin (40 μM) to scavenge hydroxyl radicals, ESR spectrometry was performed. In the Fenton reaction ($Fe^{2+}+H_2O_2 \rightarrow Fe^{3+}+\bullet OH+OH^-$), DMPO/•OH adducts generated a signal of 2,915 in control cells and this was reduced to 1,803 in the presence of galangin (Fig. 2C). Next, the intracellular ROS scavenging activity of galangin was assessed using the DCF-DA fluorescent probe. Galangin scavenged 27% of ROS (versus 52% for NAC) in H_2O_2-treated cells and 27% of ROS (versus 22% for NAC) in UVB-treated cells (Fig. 2D). Taken together, these results show that galangin efficiently scavenges ROS.

Galangin significantly attenuates UVB-induced damage of cellular macromolecules

We next investigated whether galangin can protect macromolecules, such as DNA, lipids, and proteins, from UVB-induced oxidative damage. First, UVB-induced DNA damage and the protective effects of galangin were studied using the comet assay. Representative microscopy images indicating the length of comet tails and the percentage of fluorescence in the tails are shown in Fig. 3A. UVB treatment increased

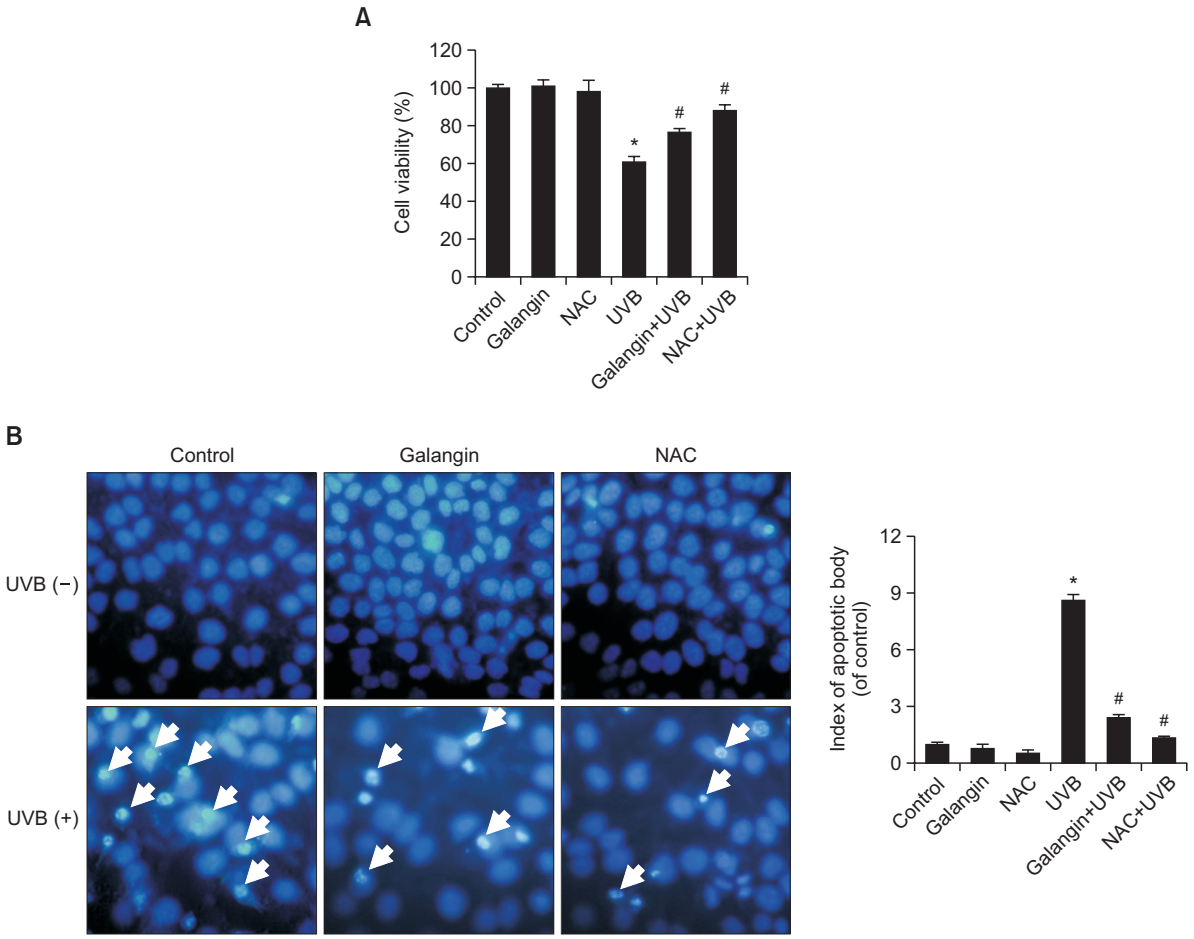

Fig. 4. Galangin increases the viability of UVB-irradiated cells and reduces apoptosis. Cells were pretreated with 40 μM of galangin and exposed to UVB (30 mJ/cm^2) 1 hour later. (A) After 24 hours, the MTT assay was performed. *Significantly different from control cells (p<0.05); #significantly different from UVB only-exposed cells (p<0.05). (B) Cells were stained with Hoechst 33342 and observed by fluorescence microscopy. The ratio between apoptotic bodies (arrows) and total number of cells were determined within randomly selected 0.3 mm^2 area of each well. *Significantly different from control cells (p<0.05); #significantly different from UVB only-exposed cells (p<0.05). JC-1 staining was performed to observe the mitochondrial membrane potential *via* (C) confocal microscopy and (D) flow cytometry. (E) Western blot analysis was performed to detect the expression levels of cleaved caspase-9, -3, Bcl-2 and Bax proteins. (Continued on 170page)

the comet tail length and increased the percentage of fluorescence in the tail to 52%, indicating an increased level of DNA damage in keratinocytes, while galangin pretreatment significantly reduced this to 34%. UVB-induced cellular membrane damage was measured by detecting lipid peroxidation *via* colorimetric determination of the level of 8-isoprostane secreted into the culture medium by HaCaT cells. The concentration of 8-isoprostane was 219 pg/ml in the culture medium of UVB-exposed cells and 32 pg/ml in that of cells pretreated with galangin prior to UVB exposure (Fig. 3B). Finally, protein carbonylation was measured to assess the degree of protein damage. Oxidative stress usually modifies the amino acid side chains of proteins to carbonyl derivatives, which can be used to quantify protein damage caused by UVB-induced oxidative stress (Dalle-Donne, 2006). Protein carbonylation was higher in UVB-treated cells than in control cells, whereas this increase was significantly reduced in cells pretreated with galangin prior to UVB exposure (Fig. 3C). These findings confirm that galangin can protect cellular macromolecules from UVB-induced oxidative damage.

Galangin reduces UVB-induced apoptosis

The viability of HaCaT cells was assessed using the MTT assay (Fig. 4A). UVB exposure reduced the viability of keratinocytes to 60% in comparison to that of control cells. However, pretreatment with galangin increased cell viability to 76%, while pretreatment with the well-known antioxidant NAC increased cell viability to 88%. Next, cells were stained with Hoechst 33342 to visualize nuclear condensation and the formation of apoptotic bodies, which are characteristic of apoptosis. Normal nuclei were observed in control and galangin-treated cells, whereas notable nuclear condensation was found in UVB-exposed cells (Fig. 4B). The nuclear condensation was significantly lowered in galangin- and NAC-pretreated cells than in UVB only-exposed cells. Mitochondrial membrane permeability plays a crucial role in the mitochondria-mediated apoptosis pathway. To elucidate the mechanism underlying how galangin protects keratinocytes against UVB-induced apoptosis, changes in the mitochondrial membrane potential were assessed. UVB treatment strongly increased the level of green fluorescence caused by JC-1 monomers, indicat-

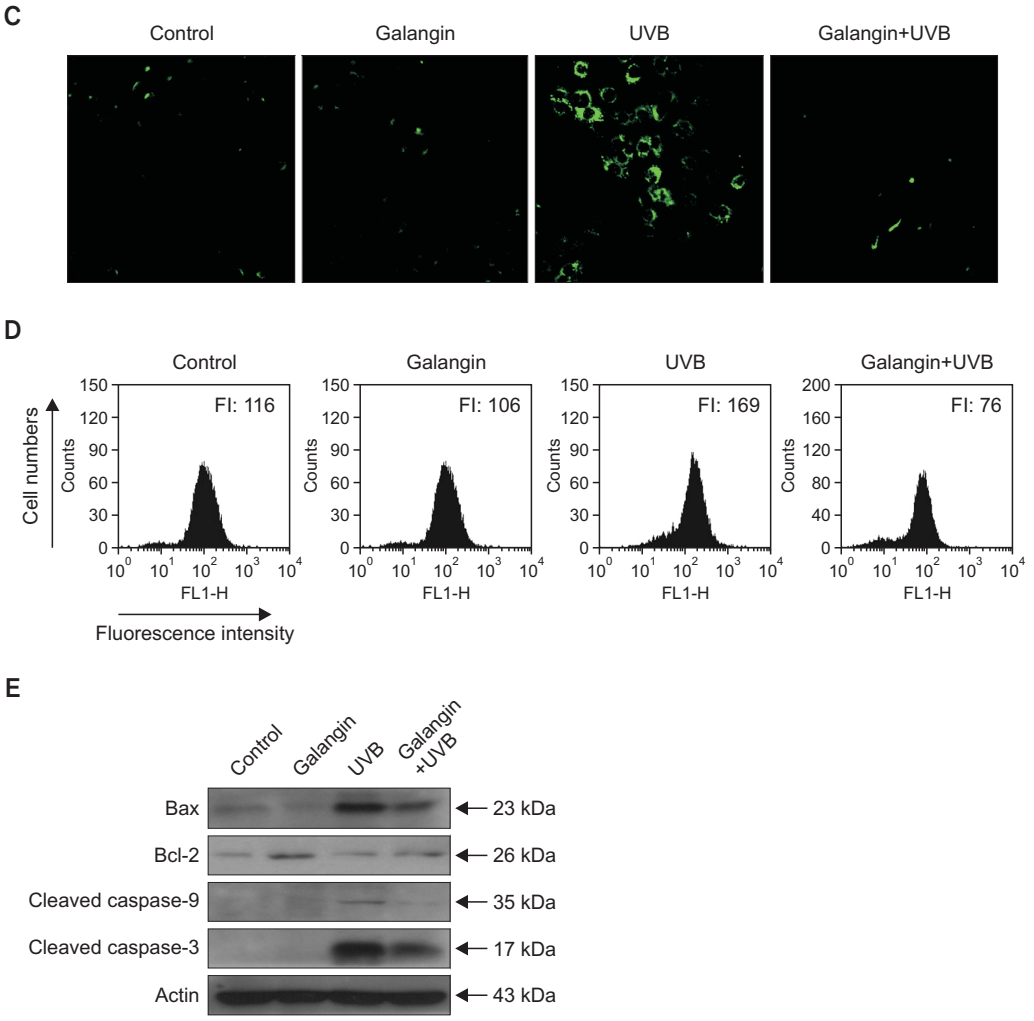

Fig. 4. Continued.

ing mitochondrial depolarization (Fig. 4C). However, galangin treatment prior to UVB exposure significantly reduced the intensity of green fluorescence, showing that galangin attenuated UVB-induced mitochondrial depolarization. To confirm these results, flow cytometric analysis of JC-1 was performed. As expected, the green fluorescence peak was increased in UVB-treated cells. However, galangin pretreatment notably reduced the peak of this fluorescence (Fig. 4D). Caspase-9, an initiator caspase, is cleaved to activate followed by the releasing cytochrome c from the depolarized mitochondria into the cytosol, cleaved caspase-9 propagates further activation of downstream apoptotic proteins which causes for cleavage of procaspase-3, activated caspase-3 triggers the apoptotic process (Adrain and Martin, 2001). To assess the caspase-9 and -3 expression levels, a western blot analysis was performed. UVB exposure resulted up-regulation of cleaved caspase-9 and -3 in HaCaT cells, interestingly galangin pretreatment significantly down-regulated the levels of cleaved caspase-9 and -3. The vulnerability of cells towards apoptosis is ultimately determined by the pro-apoptotic and anti-apoptotic proteins in the B-cell leukaemia/lymphoma-2 (Bcl-2) family (Basu and Haldar, 1998). Bcl-2 itself is consider as an anti-apoptosis protein while Bcl-2-associated x protein (Bax) is known as a pro-apoptotic protein in the Bcl-2 protein family (Wei *et al*., 2001) Therefore we next investigated the level of Bcl-2 and Bax proteins after galangin treatment (Fig. 4E). Galangin treatment prior to UVB exposure resulted up-regulation of Bcl-2 proteins whereas down- regulation of Bax proteins. These results indicate that galangin inhibits apoptotic process *via* establishing mitochondrial membrane polarity and regulating apoptotic proteins.

DISCUSSION

Chronic solar UVB exposure, also known as photoaging, is the most well understood skin aging mechanism (Nichols and Katiyar, 2010; Svobodova and Vostalova, 2010). Although the skin possesses a complex enzymatic and non-enzymatic defense system to protect it from adverse effects, prolonged UVB exposure can overwhelm this system. Solar UVB radiation has become one of the most common carcinogens in the environment and excessive UVB exposure leads to skin cancer. Meanwhile, due to the depletion of the stratospheric ozone

layer and climate change, the earth receives elevated levels of UV radiation (De Gruijl *et al*., 2003; Diffey, 2004). UVB damages DNA directly *via* the formation of pyrimidine dimers and indirectly *via* ROS generation (Ichihashi *et al*., 2003). DNA is the chief information molecule in the cell; therefore, nuclear DNA must exist for the entire life time of the cell. DNA damage can critically affect cellular functions. ROS attack not only nucleic acids but also proteins and lipids, thereby interrupting cellular metabolism. In this regard, prevention of the adverse effects caused by exposure to harmful UV radiation has become a popular theme in the cosmetic and pharmaceutical industries. Phytochemicals are well-known for their abilities to protect the skin against harmful UV radiation. Galangin is a flavone whose antioxidant ability depends on the donation of hydrogen atoms to free radicals (Sim *et al*., 2007). In this study, galangin scavenged DPPH radicals and hydroxyl radicals (Fig. 2B, C). DCF-DA staining revealed that intracellular ROS generated *via* H_2O_2 and UVB (Fig. 2D) were removed by galangin. Flavonoid is known to possess antioxidant activity by donation of a hydrogen to radicals, depending on the substitution pattern of hydroxyl groups. Hydroxylated position is related with stability of the resulting phenoxyl radical by hydrogen donation or electron delocalization. The presence of 3-OH and 5-OH and C2-C3 double bond conjugated with the 4-oxo function increase antioxidant activity (Rice-Evans *et al*., 1996; Jung *et al*., 2005). In general, O-dihydroxyl groups known as catechol structure in B ring increases radical scavenging activity, however it is reported that absence of catechol structure in the B ring like galangin is not always related with low antioxidant activity by compensating lack of catechol structure through combination C2-C3 double bond with the 3-OH and 4-keto group (Amic *et al*., 2003), demonstrating antioxidant effect as shown in our results.

UVB-induced ROS cause oxidative damage to DNA, lipids, and proteins in keratinocytes. Formation of CPDs and 6-4 photoproducts are considered as the main types of lesions caused by UVB radiation in DNA, and these adducts cause DNA strand breaks and induction of mutations (You *et al*., 2000). ROS especially hydroxyl radicals abstract allylic hydrogen forming carbon centered lipid radicals which will rapidly react with oxygen to form lipid peroxy radicals, interestingly these peroxy radicals are capable of abstract hydrogens from another lipid molecules generating lipid radicals initiating chain reactions (Ayala *et al*., 2014). ROS attack proteins and cause reversible and/or irreversible modifications, such as protein carbonylation, formation of adducts with lipid peroxidation products and protein protein cross-linking (Perluigi *et al*., 2010). Formation of protein carbonyls could be either by oxidative cleavage of proteins or by direct oxidation of lysine, arginine, proline, and threonine residues (Sander *et al*., 2002). The comet assay showed that galangin significantly suppressed DNA strand breaks induced by UVB (Fig. 3A). Detection of 8-isoprostane released by cells into the extracellular environment is an accurate means of assaying lipid peroxidation. Galangin-pretreated cells showed notably lower levels of 8-isoprostane in the culture medium than UVB alone-treated cells (Fig. 3B), suggesting that galangin attenuated UVB-induced lipid peroxidation in skin cells. Proteins are oxidized by ROS and formation of protein carbonyls is a hallmark of oxidative stress. Our results illustrated that the level of carbonyls was significantly attenuated in cells pretreated with galangin prior to UVB exposure (Fig. 3C).

At elevated concentration of ROS overwhelms the antioxidant defense system and interrupts cellular metabolism. In response to DNA damage, cells can undergo apoptosis (Barzilai and Yamamoto, 2004).

Recent studies show that UVB induced cell death is basically governed through apoptotic pathway (Ji *et al*., 2012). In addition to DNA damage and cell cycle arrest by UVB induced oxidative stress, following the membrane damage *via* lipid peroxidation and protein carbonylation, ROS weaken the inner cellular structures especially mitochondrial membranes which causes to release cytochrome c into the cytosol and activates apoptotic proteins (Kulms *et al*., 2002). Galangin pretreatment significantly increased the viability of UVB-exposed cells (Fig. 4A). Hoechst 33342 staining revealed that galangin pretreatment effectively reduced the formation of apoptotic bodies and DNA condensation induced by UVB exposure (Fig. 4B). Furthermore, we investigated the impact of galangin pretreatment on mitochondria-mediated apoptosis *via* JC-1 staining. Confocal microscopy (Fig. 4C) and flow cytometric (Fig. 4D) analyses confirmed that galangin restored mitochondrial membrane polarization. These data showed that galangin reduced apoptosis of UVB-radiated cells by establishing mitochondrial polarization. Pro-apoptotic protein Bax and anti-apoptotic protein Bcl-2 regulate the release of cytochrome c into the cytosol (Atan *et al*., 1999). Caspases are synthesized in their inactive forms in the cells and activated in respond to apoptotic signals (Thornberry and Lazebnik, 1998). Released cytochrome c into the cytosol binds to apoptotic protease activating factor 1, which then activates caspase-9 by cleaving procaspase-9 (Bossy-Wetzel *et al*., 1998). Cleaved caspase-9 activates caspase-3 and which then triggers downstream caspase cascades to execute apoptosis (Soengas *et al*., 1999). Our results elucidated that galangin suppressed the expression of Bax, cleaved caspase-9 and -3 while increased the expression of Bcl-2 protein level (Fig. 4E).

In summary, our results confirmed that galangin possesses antioxidant properties and it interferes intrinsic pathway of apoptosis *via* down regulating key apoptotic proteins, which it protected HaCaT cells from UVB-induced oxidative damage.

ACKNOWLADGMENTS

This work was supported by a National Research Foundation of Korea Grant funded by the Korean Government (MEST) (NRF-C1ABA001-2011-0021037).

REFERENCES

Adrain, C. and Martin, S. J. (2001) The mitochondrial apoptosome: a killer unleashed by the cytochrome seas. *Trends Biochem. Sci*. **26**, 390-397.

Afolayan, A. J. and Meyer, J. J. (1997) The antimicrobial activity of 3,5,7-trihydroxyflavone isolated from the shoots of *Helichrysum aureonitens*. *J. Ethnopharmacol.* **57**, 177-181.

Afolayan, A. J., Meyer, J. J., Taylor, M. B. and Erasmus, D. (1997) Antiviral activity of galangin isolated from the aerial parts of *Helichrysum aureonitens*. *J. Ethnopharmacol.* **56**, 165-169.

Amic, D., Davidovic-Amic, D., Beslo, D. and Trinajstic, N. (2003) Structure-radical scavenging activity relationships of flavonoids. *Croatica Chemica Acta* **76**, 55-61.

Atan, G., James, M. M. and Stanley, J. K. (1999) Bcl-2 family members and the mitochondria in Apoptosis. *Genes Dev.* **13**, 1899-1911.

Ayala, A. Muñoz, M. F. and Argüelles, S. (2014) Lipid peroxidation: production, metabolism, and signaling mechanisms of malondialdehyde and 4-hydroxy-2-nonenal. *Oxid. Med. Cell. Longev.* **2014**, 360438-360469.

Barzilai, A. and Yamamoto, K. (2004) DNA damage responses to oxidative stress. *DNA Repair* 1109-1115.

Basu, A. and Haldar, S. (1998) The relationship between Bcl-2, Bax and p53: consequences for cell cycle progression and cell death. *Mol. Hum. Reprod.* **4**, 1099-1109.

Beauchamp, M. C., Letendre, E. and Renier, G. (2002) Macrophage lipoprotein lipase expression is increased in patients with heterozygous familial hypercholesterolemia. *J. Lipid Res.* **43**, 215-222.

Bossy-Wetzel, E., Newmeyer, D. D. and Green, D. R. (1998) Mitochondrial cytochrome c release in apoptosis occurs upstream of DEVD-specific caspase activation and independently of mitochondrial transmembrane depolarization. *EMBO J.* **17**, 37-49.

Caldwell, M. M., Bornman, J. F., Ballare, C. L., Flint, S. D. and Kulandaivelu, G. (2007) Terrestrial ecosystems, increased solar ultraviolet radiation and interactions with other climate change factors. *Photochem. Photobiol Sci.* **6**, 252-266.

Carmichael, J., De Graff, W. G., Gazdar, A. F., Minna, J. D. and Mitchell, J. B. (1987) Evaluation of a tetrazolium-based semiautomated colorimetric assay assessment of chemosensitivity testing. *Cancer Res.* **47**, 936-942.

Ciolino, H. P. and Yeh, G. C. (1999) The flavonoid galangin is an inhibitor of CYP1A1 activity and an agonist/antagonist of the aryl hydrocarbon receptor. *Br. J. Cancer* **79**, 1340-1346.

Cossarizza, A., Baccarani-Contri, M., Kalashnikova, G. and Franceschi, C. (1993) A new method for the cytofluorimetric analysis of mitochondrial membrane potential using the J-aggregate forming lipophilic cation 5′,6′-tetrachloro-1′,3′-tetraethylbenzimidazolcarbocy anine iodide (JC-1). *Biochem. Biophys. Res. Commun.* **197**, 40-45.

Cunningham, M. L., Krinsky, V., Giovanazzi, S. M. and Peak, M. J. (1985) Superoxide anion is generated from cellular metabolites by solar radiation and its components. *J. Free Radic. Biol. Med.* **1**, 381-385.

Cushnie, T. P. T. and Lamb, A. J. (2005) Detection of galangin-induced cytoplasmic membrane damage in *Staphylococcus aureus* by measuring potassium loss. *J. Ethnopharmacol.* **101**, 243-248.

Cushnie, T. P. T. and Lamb, A. J. (2006) Assessment of the antibacterial activity of galangin against 4-quinolone resistant strains of *Staphylococcus aureus*. *Phytomedicine.* **13**, 187-191.

Dalle-Donne, I, Aldini, I., Carini, G., Colombo, M., Rossi, R. and Milzani, R. (2006) Protein carbonylation, cellular dysfunction, and disease progression. *J. Cell. Mol. Med.* **10**, 389-406.

De Gruijl, F. R., Longstreth, J., Norval, M., Cullen, A. P., Slaper, H., Kripke, M. L., Takizawa, Y. and Van der Leun, J. C. (2003) Health effects from stratospheric ozone depletion and interactions with climate change. *Photochem. Photobiol. Sci.* **2**, 16-28.

Dhumrongvaraporn, A. and Chanvorachote, P. (2013) Kinetics of ultraviolet B irradiation-mediated reactive oxygen species generation in human keratinocytes. *J. Cosmet. Sci.* **64**, 207-217.

Diffey, B. (2004) Climate change, ozone depletion and the impact on ultraviolet exposure of human skin. *Phys. Med. Biol.* **49**, R1-R11.

Donawho, C. K., Muller, H. K., Bucana, C. D. and Kripke, M. L. (1996) Enhanced growth of murine melanoma in ultraviolet-irradiated skin is associated with local inhibition of immune effector mechanisms. *J. Immunol.* **157**, 781-786.

Hattori, Y., Nishigori, C., Tanaka, T., Uchida, K., Nikaido, O., Osawa, T., Hiai, H., Imamura, S. and Toyokuni, S. (1996) 8-Hydroxy-2'-deoxyguanosine is increased in epidermal cells of hairless mice after chronic ultraviolet B exposure. *J. Invest. Dermatol.* **107**, 733-737.

Ichihashi, M., Ueda, M., Budiyanto, A., Bito, T., Oka, M. and Fukunaga, M. (2003) UV-induced skin damage. *Toxicology* **189**, 21-39.

Ikehata, H. and Ono, T. (2011) The mechanisms of UV mutagenesis. *J. Radiat. Res.* **52**, 115-125.

Ji, C. Yang, B. Yang, Z. Tu, Y. Yang, Y.L. He, L. and Bi, Z.G. (2012) Ultra-violet B (UVB)-induced skin cell death occurs through a cyclophilin D intrinsic signaling pathway. *Biochem. Biophys. Res. Commun.* **425**, 825-829.

Jung, C. H., Seog, H. M., Choi, I. W. and Cho, H. Y. (2005) Antioxidant activities of cultivated and wild Korean ginseng leaves. *Food Chem.* **92**, 535-540.

Kulms, D. Zeise, E. Poppelmann, B. and Schwarz, T. (2002) DNA damage, death receptor activation and reactive oxygen species contribute to ultraviolet radiation-induced apoptosis in an essential and independent way. *Oncogene*. **21**, 5844-5851.

Li, L., Abe, Y., Kanagawa, K., Usui, N., Imai, K., Mashino, T., Mochizuki, M. and Miyata, N. (2004) Distinguishing the 5,5-dimethyl-1-pyrroline N-oxide (DMPO)-OH radical quenching effect from the hydroxyl radical scavenging effect in the ESR spin-trapping method. *Anal. Chim. Acta* **512**, 121-124.

Lyons, N. M. and O'Brien, N. M. (2002) Modulatory effects of an algal extract containing astaxanthin on UVA-irradiated cells in culture. *J. Dermatol. Sci.* **30**, 73-84.

Matsumura, Y. and Ananthaswamy, H. N. (2004) Toxic effects of ultraviolet radiation on the skin. *Toxicol. Appl. Pharmacol.* **195**, 298-308.

Meeran, S.M., Punathil, T. and Katiyar, S. K. (2008) Interleukin-12-deficiency exacerbates inflammatory responses in UV irradiated skin and skin tumors. *J. Invest. Dermatol.* **128**, 2716-2727.

Nichols, J. A. and Katiyar, S. K. (2010) Skin photoprotection by natural polyphenols: anti-inflammatory, antioxidant and DNA repair mechanisms. *Arch. Dermatol. Res.* **302**, 71-83.

Park, H. M., Kim, H. J., Jang, Y. P. and Kim, S. Y. (2013) Direct analysis in real time mass spectrometry (DART-MS) analysis of skin metabolome changes in the ultraviolet B-induced mice. *Biomol Ther.* **21**, 470-475.

Perluigi, M. Di Domenico, F. Blarzino, C. Foppoli, C. Cini, C. Giorgi, A. Grillo, C. De Marco, F. Butterfield, D. A. Schinin , M. E. and Coccia, R. (2010) Effects of UVB induced oxidative stress on protein expression and specific protein oxidation in normal human epithelial keratinocytes: a proteomic approach. *Proteome Sci.* **8**, 13.

Rajagopalan, R., Ranjan, S. K. and Nair, C. K. (2003) Effect of vinblastine sulfate on gamma-radiation-induced DNA single-strand breaks in murine tissues. *Mutat Res.* **536**, 15-25.

Rice-Evans, C. A., Miller, N. J. and Paganga, G. (1996) Structure-antioxidant activity relationships of flavonoids and phenolic acids. *Free Radic. Biol. Med.* **20**, 933-956.

Rosenkranz, A. R., Schmaldienst, S., Stuhlmeier, K. M., Chen, W., Knapp, W. and Zlabinger, G. J. (1992) A microplate assay for the detection of oxidative products using 2',7' dichlorofluorescin-diacetate. *J. Immunol. Methods* **156**, 39-45.

Sander, C. S., Chang, H., Salzmann, S., Müller, C. S., Ekanayake-Mudiyanselage, S., Elsner, P. and Thiele, J. J. (2002) Photoaging is associated with protein oxidation in human skin *in vivo*. *J. Invest. Dermatol.* **118**, 618-625.

Sim, G., Lee, B., Ho, S. C., Jae, W. L., Kim, J., Lee, D. H., Kim, J. H., Pyo, H. B., Moon, D. C., Oh, K. W., Yun, Y. P. and Hong, J. T. (2007) Structure activity relationship of antioxidative property of flavonoids and inhibitory effect on matrix metalloproteinase activity in UVA-irradiated human dermal fibroblast. *Arch. Pharm. Res.* **30**, 290-298.

Singh, N. P. (2000) Microgels for estimation of DNA strand breaks, DNA protein crosslinks and apoptosis. *Mutat. Res.* **455**, 111-127.

So, F. V., Guthrie, N., Chambers, A. F., Moussa, M. and Carroll, K. K. (1996) Inhibition of human breast cancer cell proliferation and delay of mammary tumorigenesis by flavonoids and citrus juices. *Nutr. Cancer* **26**, 167-181.

Soengas, M. S., Alarcon, R. M., Yoshida, H., Giaccia, A. J., Hakem, R., Mak, T. W. and Lowe, S. W. (1999) Apaf-1 and caspase-9 in p53-dependent apoptosis and tumor inhibition. *Science* **284**, 156-159.

Sumiyoshi, M. and Kimura, Y. (2009) Effects of a turmeric extract (*Curcuma longa*) on chronic ultraviolet B irradiation-induced skin damage in melanin-possessing hairless mice. *Phytomedicine* **16**, 1137-1143.

Svobodova, A. and Vostalova, J. (2010) Solar radiation induced skin damage: review of protective and preventive options. *Int. J. Radiat. Biol.* **86**, 999-1030.

Thornberry, N. A. and Lazebnik, Y. (1998) Caspases: Enemies within. *Science* **281**, 1312-1316.

Troiano, L., Ferraresi, R., Lugli, E., Nemes, E., Roat, E., Nasi, M., Pinti, M. and Cossarizza, A. (2007) Multiparametric analysis of cells with different mitochondrial membrane potential during apoptosis by polychromatic flow cytometry. *Nat Protoc.* **2**, 2719-2727.

Tsoyi, K., Park, H. B., Kim, Y. M., Chung, J. I., Shin, S. C., Shim, H. J., Lee, W. S., Seo, H. G., Lee, J. H., Chang, K. C. and Kim, H. J. (2008) Protective effect of anthocyanins from black soybean seed coats on UVB induced apoptotic cell death *in vitro* and *in vivo*. *J. Agric. Food Chem.* **56**, 10600-10605.

Wei, M. C., Zong, W. X., Cheng, E. H., Lindsten, T. P. V., Roth, K. A., MacGregor, G. R., Thompson, C. B. and Korsmeyer, S. J. (2001) Proapoptotic BAX and BAK: a requisite gateway to mitochondrial dysfunction and death. *Science* **292**, 727-730.

Yoshikawa, T., Rae, V., Bruins-Slot, W., Van den Berg, J. W., Taylor, J. R. and Streilein, J. W. (1990) Susceptibility to effects of UVB radiation on induction of contact hypersensitivity as a risk factor for skin cancer in humans. *J. Invest. Dermatol.* **95**, 530-536.

You, H. Y. Szabo, P. E. and Pfeifer, G. P. (2000) Cyclobutane pyrimidine dimers form preferentially at the major p53 mutational hotspot in UVB-induced mouse skin tumors. *Carcinogenesis.* **21**, 2113-2117.